Analog Interference Cancellation for Full-Duplex Broadband Power Line Communications

Gautham Prasad, Lutz Lampe, and Sudip Shekhar
Department of Electrical and Computer Engineering
The University of British Columbia, Vancouver, BC
Email: gauthamp@ece.ubc.ca

***Abstract*—In this paper, we present an all-analog echo cancellation solution to achieve in-band full-duplex (IBFD) operation in broadband power line communications (BB-PLC). The performance of active digital interference cancellation, as proposed previously for IBFD BB-PLC, is limited by distortion and quantization noise introduced by the analog-to-digital converter (ADC). Hence, we explore analog interference cancellation (AIC) solutions to reduce the power of the signal entering the ADC. We consider various AIC solutions for other communication media known from the literature, and show that a direct implementation of any of these solutions to a BB-PLC system renders an expensive and/or ineffective realization. Acknowledging the specific challenges encountered in BB-PLC, we propose an AIC mechanism that not only eliminates the effects of ADC distortion and quantization noise, but also provides sufficient echo cancellation gain (ECG) to function without an active digital interference cancellation module. We demonstrate through simulation results that our proposed solution provides over 80 dB of ECG, which is sufficient to reduce the echo power down to the minimum power line noise floor.**

***Index Terms*—Analog cancellation, in-band full-duplex (IBFD), broadband power line communication (BB-PLC), echo cancellation.**

I. Introduction and Motivation

In-band full-duplex (IBFD) operation provides broadband power line communication (BB-PLC) systems the ability to simultaneously transmit and receive data in the same frequency band over the same power line. Apart from doubling physical layer transfer rates without additional power or bandwidth requirements, IBFD also provides several higher layer benefits [1], [2]. IBFD can be achieved by canceling the interfering transmitted signal component from the received signal, to effectively comprehend the signal-of-interest (SOI). This cancellation is achieved by using echo/self-interference (SI) cancellation techniques that have been used in various full-duplex systems across different communication media [2]–[8].

Echo cancellation (EC) schemes can be broadly categorized into analog and digital cancellation techniques. Analog cancellation operates on analog signals either before or after the transmitted signal interferes with the SOI. Analog isolation that is applied on the self-transmitted signal before it enters the receiver chain is commonly referred to as passive isolation [2]. On the other hand, active cancellation techniques regenerate and cancel an estimate of the transmitted signal component from the received signal inside the receiver. Since digital interference cancellation (DIC) can only be applied on the signal after analog-to-digital conversion, DIC techniques are always active cancellation solutions.

In our earlier works, we proposed an IBFD solution for BB-PLC, with passive analog isolation using an operational amplifier (op-amp) based hybrid, and an adaptive active DIC procedure [1], [9]. Although this solution achieved 75% median data rate gains (DRGs) under typical in-home PLC channel and noise conditions, the maximum EC gain (ECG) obtained was limited by the quantization noise and distortion (NAD) introduced by the analog-to-digital converter (ADC). Therefore, we examine the applicability of an additional analog interference cancellation (AIC) module, either as a passive or an active cancellation solution, to eliminate the limiting effect of NAD.

In this paper, we first investigate the suitability of the known AIC methods that have been implemented in full-duplex systems across different communication media. An examination of each of these schemes reveals that none of the available AIC solutions can be directly adopted for BB-PLC scenarios to obtain an efficient implementation. Therefore, we propose an AIC solution in which we perform echo estimation digitally, but cancel the echo in the analog domain. In this way, we augment the benefits of digital computation with achieving the goal of analog EC. Our simulation results indicate that our proposed solution potentially provides sufficient ECG to reduce the power spectral density (PSD) of the echo down to that of the noise floor at the receiver. Therefore, our AIC technique can function independently without an additional active DIC module. As a result, we present the first *all-analog* EC solution for IBFD BB-PLC systems, where passive isolation is achieved using an op-amp based hybrid, and active cancellation through an adaptive AIC module.

The rest of the paper is organized as follows. In Section II, we present a discussion on the constraints imposed by BB-PLC for an efficient AIC implementation using the available AIC techniques. To effectively address these restrictions, we propose a digitally controlled AIC method in Section III. We present numerical results in Section IV, with simulations performed under realistic BB-PLC channel and noise conditions. Section V concludes the paper.

This work was supported by the Natural Sciences and Engineering Research Council of Canada (NSERC).

II. Analog Cancellation Techniques

In this section, we examine the applicability of various existing passive and active AIC techniques to a BB-PLC scenario.

A. Analog Passive Cancellation

Passive cancellation is typically performed on the echo signal during its propagation into the receiver chain, in order to minimize the echo component interfering with the SOI. Recent advances in passive isolation techniques have mainly been in wireless IBFD systems. These propagation domain cancellations are implemented differently for single- and multiple-antenna scenarios. For a multiple-antenna single-input single-output (SISO) configuration that uses separate antennas for transmission (TX) and reception (RX), passive isolation techniques such as antenna spacing, antenna separation, or antenna isolation are commonly used [10]–[14]. These techniques involve determining the placement of TX and RX antennas in order to minimize the echo interference. For example, antenna separation recommends placing the TX and RX antennas as far away as possible from each other to maximize path loss during propagation [13]. Alternatively, antenna isolation can be achieved by, say, directional isolation, where the TX and RX antennas exploit spatial diversity to increase passive isolation [14]. However, PLC does not possess the physical flexibility to vary antenna positions, due to the manner in which PLC data is coupled on to the power line [15]. Although, multi-antenna-like passive isolation can be achieved by using separate conductor-pairs for transmission and reception to exploit the coupling loss between the two pairs. But such a solution doubles the resources used to achieve a SISO operation. Therefore, we use a single-antenna (conductor-pair) transceiver, and persist with the analog passive isolation solution proposed in [9] using an active hybrid circuit.

B. Analog Active Cancellation

1) AIC using Delay Lines: An active AIC solution was proposed in [16] for wireless IBFD systems to reconstruct the echo using analog weights and delays. A portion of the transmitted analog signal was passed through a dedicated set of delay lines of varying lengths to obtain the signal with different delays. However, such a solution is impractical for BB-PLC scenarios, as the frequency selective nature of the network impedance results in reflected echoes consisting of multiple notable components that requires large number of lengthy delay lines. Furthermore, this solution requires pauses in transmission to configure the weights and delays to changing echo channel conditions. In a BB-PLC scenario, the echo channel varies with changing power line network impedance. This would require frequently resetting the weights and delays to adapt to the quickly changing channel conditions. Hence, AIC using delay lines is not applicable to BB-PLC.

2) Adaptive Cancellation with Analog LMS Filter: Some of the first implementations of adaptive AIC are found for full-duplex Ethernet and co-axial cable transmissions [6], [7]. These solutions apply an analog finite impulse response (FIR) filter and adaptively tune its filter weights to estimate the impulse response of the echo channel. For example, the implementation in [7] uses a four-tap filter to cancel the four most significant echo samples. But we have shown earlier in [9] that due to multiple significant reflections along the power line, the echo channel estimation filter requires at least 40 taps to completely capture the channel effects. Hence, we require 40 additional digital-to-analog converters (DACs) to use the structure of [7], as it uses the digital samples of the transmitted signal for echo reconstruction. Alternatively, to avoid the use of multiple DACs, the solution of [6], and a similar wireless-IBFD implementation in [17], use the analog transmitted signal to generate an echo estimate. However, since these solutions use analog FIR filters for channel estimation, it provides inefficient reconfiguration of filter weights and delays to frequently changing channel conditions, as is experienced in BB-PLC networks. Therefore, it is preferable to use a solution that can implement AIC with the aid of digital processing to provide superior adaptivity and reconfigurability.

3) Digitally Controlled AIC: An AIC solution with digital echo channel estimation was proposed in [18], and was later extended to broader bandwidth applications in [13], [19]. These solutions use the digital samples of the transmitted signal to generate a canceling signal by estimating the frequency response of the echo channel. Such a solution provides the benefits of digital channel estimation and a reduced NAD due to AIC. However, they require an entire additional transmitter chain for echo reconstruction. Additionally, these solutions require a rather long wait-time/silent period for echo channel estimation, where the transceiver operates in HD mode. An analogous solution was also proposed in [20], albeit with similar drawbacks as those faced by [13], [18], [19]. Thus, an adaptive echo estimator with a simpler echo reconstruction chain is desirable.

In the following, we propose a digitally controlled adaptive AIC solution that is suitable for BB-PLC, in particular, considering coupling of PLC signals, adaptivity to frequently varying echo channel conditions, and low implementation complexity and power consumption.

III. Proposed Solution

We consider a single-antenna BB-PLC transceiver and apply the op-amp based hybrid circuit of [9] for passive AIC. For active cancellation, we propose the following AIC technique aided by digital echo channel estimation.

A. AIC Procedure

Consider a BB-PLC transceiver shown in Fig. 1, which transmits an orthogonal frequency division multiplexed (OFDM) signal, x, and receives a signal, y, which contains the

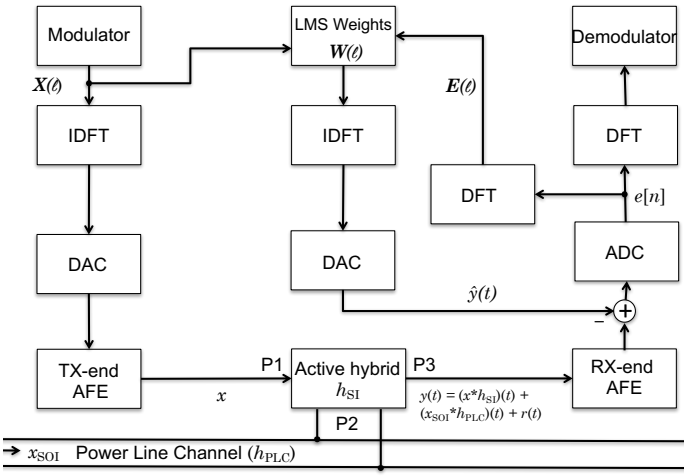

Fig. 1. A block diagram of an IBFD BB-PLC transceiver with our proposed all-analog cancellation solution.

echo, SOI, and noise. The received signal can be expressed in continuous time as

$$y(t) = \underbrace{(x * h_{\mathsf{SI}})(t)}_{\text{echo}} + \underbrace{(x_{\mathsf{SOI}} * h_{\mathsf{PLC}})(t)}_{\text{SOI}} + \underbrace{r(t)}_{\text{noise}}, \tag{1}$$

where h_{SI} is the impulse response of the echo channel, x_{SOI} is the required SOI, h_{PLC} is the impulse response of the power line channel, and r is the cumulative noise seen at the receiver. An echo estimate is removed from this signal in the analog domain, and the resultant signal, $e = y - \hat{y}$, is appropriately scaled and digitized by the ADC. The digital samples, $e[n]$, are fed back to the echo channel estimator in frequency domain to adapt its filter weights for the following iteration. The filter-weight vector, $\boldsymbol{W}$, is adapted at every ℓth iteration using the least mean squares (LMS) algorithm as [21, Ch. 5]

$$\boldsymbol{W}(\ell+1) = \boldsymbol{W}(\ell) + \mu \mathrm{diag}(\boldsymbol{X}(\ell))^* \boldsymbol{E}(\ell), \tag{2}$$

where μ is the step size of the LMS algorithm, and $\boldsymbol{X}$ and $\boldsymbol{E}$ are the frequency domain versions of x and e, respectively. Since $\boldsymbol{W}$ represents the echo channel transfer function estimate, we generate the echo estimate in frequency domain as

$$\hat{\boldsymbol{Y}}(\ell) = \boldsymbol{X}(\ell) \circ \boldsymbol{W}(\ell), \tag{3}$$

where '$\circ$' denotes the Hadamard product. We then convert $\hat{\boldsymbol{Y}}$ to time domain and use a DAC to obtain the continuous time analog echo estimate. We continuously repeat this process for every ℓth OFDM block.

B. Reduction in Quantization Noise and Distortion

The NAD power introduced by the ADC is given by

$$P_{\mathsf{NAD}} = \frac{P_{\mathrm{inp}}}{\mathsf{SINAD}}, \tag{4}$$

where P_{inp} is the input power of the signal entering the ADC and SINAD is the signal-to-NAD ratio at the ADC. While SINAD is constant for a given ADC, P_{inp} is dependent on the total AIC gain, for a fixed transmit signal power, P_{TX}. When AIC is only achieved using passive isolation, as in [9],

$$P_{\mathsf{NAD}}^{(\mathrm{DIC})} = \frac{P_{\mathrm{TX}} G_{\mathrm{hyb}} + P_{\mathrm{TX}} G_{\mathsf{PLC}} + N_{\mathrm{R}}}{\mathsf{SINAD}}, \tag{5}$$

where G_{hyb} is the hybrid isolation, G_{PLC} is the power line channel gain, and N_{R} is the power of the cumulative noise floor at the receiver. Since G_{hyb} is relatively weak, NAD introduced by the ADC limits the EC performance when AIC is only achieved using the hybrid.

In our proposed solution, AIC is accomplished both passively and actively. Hence,

$$P_{\mathsf{NAD}}^{(\mathrm{AIC})}(\ell) = \frac{P_{\mathrm{TX}} G_{\mathrm{hyb}} G_{\mathrm{AIC}}(\ell) + P_{\mathrm{TX}} G_{\mathsf{PLC}} + N_{\mathrm{R}}}{\mathsf{SINAD}}, \tag{6}$$

where G_{AIC} is the active cancellation gain provided by AIC. Since AIC is implemented adaptively, G_{AIC} is dependent on the LMS iteration ℓ. As the LMS adaptation reaches saturation, it provides sufficient gain to produce $G_{\mathrm{AIC}} \approx 0$. This nullifies any effect of the echo on P_{NAD}. Therefore, the NAD introduced by the ADC no longer limits the EC performance.

C. Effect of Non-Linear SI Components

The active DIC solution of [9] could ignore the effects of non-linear SI components as $P_{\mathsf{NAD}}^{(\mathrm{DIC})}$ was more dominant. However, since $P_{\mathsf{NAD}}^{(\mathrm{AIC})} \ll P_{\mathsf{NAD}}^{(\mathrm{DIC})}$, the effects of non-linear SI components are no longer negligible. Non-linear components are mainly generated by the power amplifiers in the transmitter chain. Typical BB-PLC analog front-ends (AFEs) produce non-linear signal components that have a PSD of -75 to -80 dB below the transmit PSD, Ψ_{TX} [22]. Ψ_{TX} used by BB-PLC transceivers are determined by regulatory authorities, and varies with location. For example, North American regulations, used by HomePlug AV standards, allow $\Psi_{\mathrm{TX}} \leq -50$ dBm/Hz [23], whereas European restrictions limit $\Psi_{\mathrm{TX}} \leq -55$ dBm/Hz [24]. As the PSD of non-linear components, Ψ_{NLC}, is larger for higher Ψ_{TX}, we consider $\Psi_{\mathrm{TX}} = -50$ dBm/Hz to address the worst-case scenario. With a BB-PLC AFE such as [22], we experience $\Psi_{\mathsf{NLC}} \leq -125$ dBm/Hz. Therefore, to bring Ψ_{NLC} down to the minimum in-home power line noise floor of -130 dBm/Hz [9], we require a non-linear cancellation of up to 5 dB.

Since the echo passes through the analog hybrid before entering the receiver chain, non-linear SI components undergo passive hybrid isolation. It has been shown in [9] that the average G_{hyb} is about 7 dB. However, hybrid isolation is frequency selective due to the varying network impedance, and could be as low as 2 dB at certain frequencies. Under such network impedance conditions, Ψ_{NLC} is 3 dB above the minimum noise floor. Toward proposing a low-complexity and a low-power overhead solution, we choose to endure this outlier scenario without including any additional active non-linear cancellation.

D. Characteristics of our Proposed Solution

Our proposed AIC solution achieves the targets set in Section II. In the following, we present a brief discussion on the salient features associated with our solution.

1) Adaptive Filter Weight Update: As our proposed solution updates the weights of the echo channel estimation filter adaptively using the LMS algorithm, it inherently tracks all the variations in channel conditions without requiring any weights re-initialization. Furthermore, unlike digitally controlled AIC solutions of [18], [19], we use the received signal for filter weight adaptation in the presence of the SOI. Hence, we do not require any silent period (HD transmission) either at the beginning of transmission, or anytime thereafter. To adapt to short-term power line channel changes that are linear periodically time varying (LPTV) in nature [25], we could further incorporate the LPTV-LMS algorithm developed in [9].

2) Accuracy of the Echo Estimate: Since we use the received signal, y, as the training signal to adapt the LMS filter weights, the accuracy of the generated echo estimate depends on the power of the echo component in y. The other components in y, namely the SOI and the cumulative noise at the receiver, together act as the overall noise to the echo channel estimator. Therefore, a smaller SOI component in y provides a more accurate echo estimate. With a constant transmit PSD used by the far-end BB-PLC transceiver, the SOI power in received signal depends on the power line channel attenuation. Thus, the accuracy of the echo estimate improves as the power line channel attenuation increases.

3) Cost of Implementation: To achieve analog SI cancellation, we require an analog adder in the receiver chain. This can be implemented simply using current addition, or using an active differential voltage amplifier to ensure no additional signal power loss inside the adder. Additionally, we only require one extra DAC in the echo reconstruction chain to generate an analog echo estimate signal from the digital samples. These two analog components are elementary constituents of any digitally controlled AIC solution. Note that our proposed structure is significantly more cost and power efficient than those in [18], [19], as BB-PLC systems operate with baseband signals.

IV. Numerical Results

In this section, we present simulation results of echo cancellation and data rate gains obtained in practical IBFD BB-PLC transceivers using our proposed AIC solution.

A. Simulation Configuration

1) Transceiver Settings: We use the HomePlug AV specifications to configure our single-antenna BB-PLC transceiver [26]. We use a fast Fourier transform (FFT) of size 3072 to load data onto 917 sub-carriers between $2-28$ MHz. Intermediate sub-carriers are nulled as per the tone-mask specified in [26, Table 3-23]. We use the North American amplitude mask of [26, Figure 3-24] and set $\Psi_{\mathrm{TX}} = -50$ dBm/Hz on all sub-carriers. To simulate an analog signal of infinite precision, we use the default 64-bit double precision of MATLAB. We digitize the analog signal using a 12-bit ADC with 11 effective number of bits. We use the Hammerstein model of baseband power amplifiers to simulate the programmable gain amplifiers used in the BB-PLC transceiver [27]. We summarize the simulation parameters in Table I.

TABLE I
Simulation Parameters

Transmission bandwidth	$2-28$ MHz
Sampling frequency	75 MHz
FFT Size	3072
Sub-carrier spacing (Δf)	24.414 kHz
Number of data carrying sub-carriers ($\lvert\mathscr{N}\rvert$)	917
Transmit PSD (Ψ_{TX})	-50 dBm/Hz
ADC Resolution	12 bits

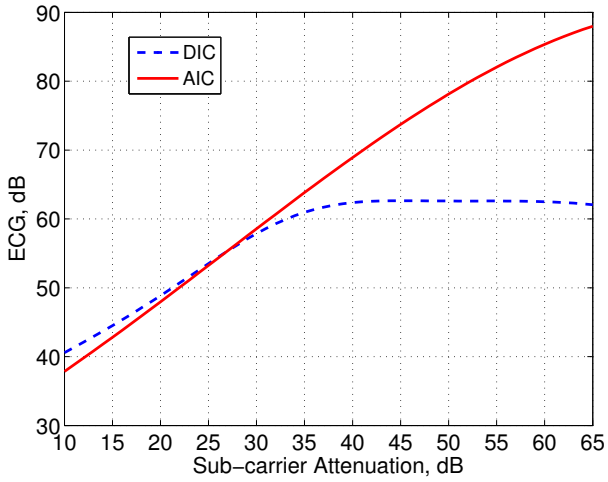

Fig. 2. A second-order Gaussian curve fit of the ECGs obtained across varying sub-carrier attenuations using the DIC IBFD implementation of [9], and our proposed AIC implementation.

2) Channel and Noise Generation: We use the channel generator in [28] to realize realistic in-home PLC channels, which computes the channel transfer function using the bottom-up approach [29]. To simulate PLC noise, we use the cumulative power line noise generator tool of [30], which generates the overall noise as a sum of colored background noise, narrowband noise, periodic impulse noise synchronous with the mains, periodic impulse noise asynchronous with the mains, and aperiodic impulse noise.

B. Echo Cancellation Gain

We define ECG as the ratio of the signal-to-interference-plus-noise ratio (SINR) before EC to SINR after EC. Thus, we can write ECG at every sub-carrier as

$$\mathsf{ECG} \approx \frac{\Psi_{\mathrm{TX}}}{\Psi_{\mathsf{RSI}} + \Psi_{\mathrm{N}}}, \tag{7}$$

where Ψ_{RSI} and Ψ_{N} are the PSDs of the residual SI (RSI) including the effects of NAD and non-linear SI components, and the noise floor at the receiver, respectively.

We run our proposed AIC solution and the IBFD solution of [9] on a BB-PLC transceiver over 1500 random PLC channels generated using the random network generator setting in [28]. To determine the maximum ECG obtainable using our proposed solution, we run our simulations under zero-noise conditions to ensure that the power line noise does not limit the achieved ECG.

Fig. 2 shows a second-order Gaussian curve-fit plot of the variation of ECG for different sub-carrier attenuations. We observe that ECG increases with increase in sub-carrier attenuation due to more accurate echo estimates, as explained in Section III-D2. The difference in ECG values between the two curves at lower sub-carrier attenuations can be attributed to discrepancies of the curve-fit. At higher attenuations, we notice that while ECG with the IBFD implementation of [9] saturates at about 63 dB due to dominating P_{NAD}, we obtain ECG of up to 85 dB with our proposed AIC solution. This exceeds the target 80 dB ECG required to bring the echo PSD down to that of the minimum receiver noise floor [9]. However, since we do not obtain $\mathsf{ECG} > 80$ dB across all sub-carrier attenuations, we do not double the overall data rate under all channel conditions.

C. Data Rate Gains

We use the ECG values of Fig. 2 to calculate the data rates obtained for realistic PLC channel and noise scenarios. We compute the data rates for HD and IBFD operations, C_{HD} and C_{FD}, respectively, as

$$C_{\mathsf{HD}} = \Delta f \cdot \sum_{k \in \mathcal{N}} \log_2 \left(1 + \frac{\Psi_{\mathrm{TX}} \cdot |H_{\mathsf{PLC}}(k)|^2}{\Psi_{\mathrm{N}}(k)}\right) \tag{8}$$

$$C_{\mathsf{FD},\phi} = 2 \cdot \Delta f \cdot \sum_{k \in \mathcal{N}} \log_2 \left(1 + \frac{\Psi_{\mathrm{TX}} \cdot |H_{\mathsf{PLC}}(k)|^2}{\Psi_{\mathsf{RSI},\phi}(k) + \Psi_{\mathrm{N}}(k)}\right), \tag{9}$$

respectively, where Δf is the OFDM sub-carrier spacing, H_{PLC} is the PLC channel transfer function, k is the sub-carrier index, $\mathcal{N}$ is the set of all data carrying sub-carriers, and $\phi = \{\mathrm{AIC}, \mathrm{DIC}\}$ indicates the chosen IBFD solution, where AIC represents our proposed AIC solution and DIC is the IBFD implementation of [9]. We calculate the RSI PSD using the values of ECG from Fig. 2 as

$$\Psi_{\mathsf{RSI},\phi}(k) = \frac{\Psi_{\mathrm{TX}}}{\mathsf{ECG}(k)}.$$

From (8) and (9), we then determine the DRG obtained using IBFD over a HD operation as

$$\mathsf{DRG}_{\phi} = \frac{C_{\mathsf{FD},\phi}}{C_{\mathsf{HD}}}. \tag{10}$$

We compute (8), (9), and (10) for four diverse in-home BB-PLC channels shown in Fig. 3. We generate these channels using [28] by configuring the PLC network with different number of derivation boxes and power outlets. We ensure that we generate channels with a range of attenuations between 10 dB and 80 dB. To introduce PLC noise, we use the power line noise generator tool of [30] with a random noise level setting.

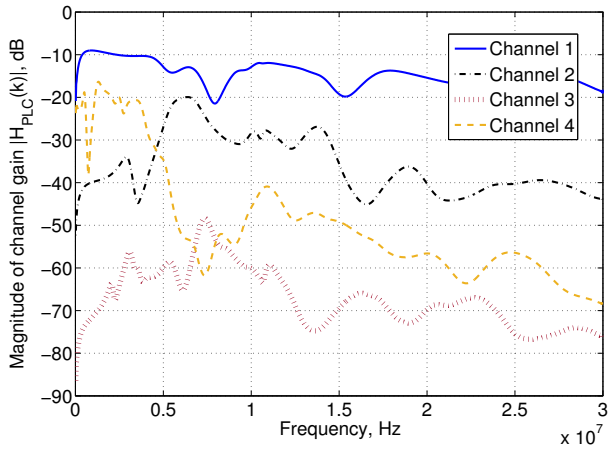

Fig. 3. Channel transfer functions of four diverse in-home BB-PLC channels.

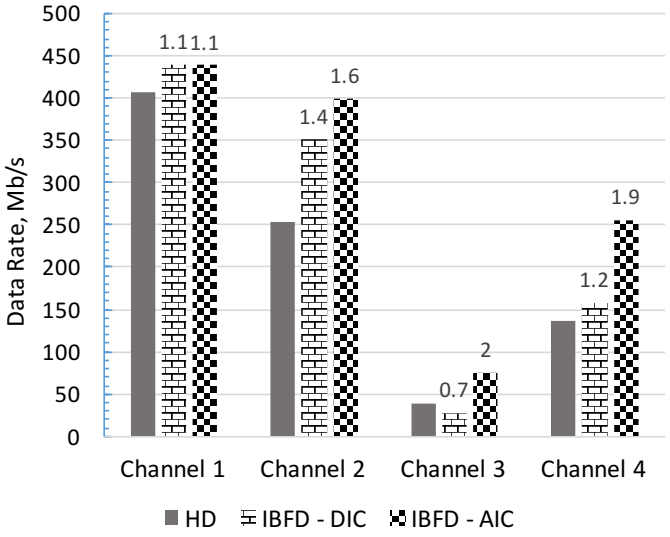

Fig. 4. Data rates obtained for the four BB-PLC channels in Fig. 3. DRG with IBFD, computed as (10), is indicated on top of each IBFD bar. Individual data rates are computed using (8) and (9).

The obtained data rates, C_{HD}, $C_{\mathsf{FD,DIC}}$, and $C_{\mathsf{FD,AIC}}$, for the four channels of Fig. 3 can be seen in Fig. 4. Additionally, the values of DRG_{ϕ} are indicated on top of the $C_{\mathsf{FD},\phi}$ bar. We observe that $C_{\mathsf{FD,AIC}} \geq C_{\mathsf{FD,DIC}}$ is consistently the case for all channels.

1) Channel 1: This channel contains a relatively low attenuation across all sub-carriers, which is characteristic of short power line links. Since the ECG obtained under lower sub-carrier attenuations is smaller, DRGs obtained under both AIC and DIC solutions are also relatively small. Notice in Fig. 2 that for attenuations below 30 dB, $\mathsf{ECG}_{\mathrm{DIC}} \approx \mathsf{ECG}_{\mathrm{AIC}}$. Thus, we obtain $C_{\mathsf{FD,AIC}} \approx C_{\mathsf{FD,DIC}}$ for this channel. However, we note that practical data rates obtained are limited by the maximum modulation order supported by the device. For example, HomePlug AV specifications support 1024-quadrature amplitude modulation as its highest order. In such cases, the

DRG_{ϕ} would be higher as C_{HD} is limited by this constraint.

2) Channel 2: This channel provides greater sub-carrier attenuation than Channel 1. Hence, we observe lesser overall data rates under all three operations. Notice from Fig. 2 that $\mathsf{ECG}_{\mathrm{DIC}}$ saturates at 63 dB beyond all attenuations of about 35 dB. As this channel contains a significant number of sub-carriers with attenuations greater than 35 dB, we obtain $C_{\mathsf{FD,AIC}} > C_{\mathsf{FD,DIC}}$.

3) Channel 3: Channel 3 presents large attenuation across all sub-carriers, which is characteristic of long power line runs with several loads connected in the network. Although such channels are not frequently encountered in typical in-home conditions, it illustrates a drawback of the IBFD implementation of [9], and its remedy using our proposed solution. As all sub-carriers in this channel provide high attenuations, $\mathsf{ECG}_{\mathrm{DIC}}$ is always saturated at a maximum value of 63 dB. This produces $C_{\mathsf{FD,DIC}} < C_{\mathsf{HD}}$, resulting in a $\mathsf{DRG}_{\mathrm{DIC}} = 0.7$. On the contrary, our AIC solution provides greater $\mathsf{ECG}_{\mathrm{AIC}}$ at higher sub-carrier attenuations. Thus, we obtain $\mathsf{DRG}_{\mathrm{AIC}} = 2$.

4) Channel 4: This channel contains a wide range of sub-carrier attenuations between 20 dB and 70 dB. Due to a constantly growing $\mathsf{ECG}_{\mathrm{AIC}}$, we obtain a $\mathsf{DRG}_{\mathrm{AIC}} = 1.9$ using our proposed solution, while $\mathsf{DRG}_{\mathrm{DIC}}$ is limited to 1.2.

V. Conclusions

In this paper, we have presented the first all-analog echo cancellation solution for full-duplex PLC. By performing active EC in the analog domain, we overcame the limitation of distortion and quantization noise introduced by the ADC. Considering the known AIC techniques available in IBFD and frequency division duplexed systems across different communication media, we proposed a digitally controlled analog cancellation solution tailored for BB-PLC scenarios. We showed through simulation results that the ECG values obtained by our solution is sufficient to function independently without an additional DIC module. Our numerical results also indicate that our all-analog cancellation solution provides greater echo cancellation gains and data rate gains compared to the state-of-the-art IBFD implementation. We remark that our active AIC solution is also easily scalable to multiple-input multiple-output BB-PLC transceivers.

References

[1] G. Prasad, L. Lampe, and S. Shekhar, "Enhancing transmission efficiency of broadband PLC systems with in-band full duplexing," in *IEEE Intl. Symp. Power Line Commun. and Its Appl. (ISPLC)*, March 2016.

[2] A. Sabharwal, P. Schniter, D. Guo, D. W. Bliss, S. Rangarajan, and R. Wichman, "In-band full-duplex wireless: Challenges and opportunities," *IEEE J. Sel. Areas Commun.*, vol. 32, no. 9, pp. 1637–1652, 2014.

[3] S. Weinstein, "Echo cancellation in the telephone network," *IEEE Commun. Mag.*, vol. 15, no. 1, pp. 8–15, January 1977.

[4] A. G. Stove, "Linear FMCW radar techniques," in *IEE Proceedings F-Radar and Signal Processing*, vol. 139, no. 5. IET, 1992, pp. 343–350.

[5] M. Ho, J. M. Cioffi, and J. A. Bingham, "Discrete multitone echo cancelation," *IEEE Trans. Commun.*, vol. 44, no. 7, pp. 817–825, 1996.

[6] R. Mahadevan, "A front-end circuit for full-duplex transmission over coaxial cable." Ph.D. dissertation, University of Toronto, 2001.

[7] T.-C. Lee and B. Razavi, "A 125-MHz mixed-signal echo canceller for gigabit ethernet on copper wire," *IEEE J. Solid-State Circuits*, vol. 36, no. 3, pp. 366–373, 2001.

[8] "IEC 62488-1:2012: Power line communication systems for power utility applications," *International Electrotechnical Commission*. [Online]. Available: https://webstore.iec.ch/publication/7095

[9] G. Prasad, L. Lampe, and S. Shekhar, "In-band full duplex broadband power line communications," *IEEE Trans. Commun.*, vol. 64, no. 9, pp. 3915–3931, Sept 2016.

[10] J. I. Choi, M. Jain, K. Srinivasan, P. Levis, and S. Katti, "Achieving single channel, full duplex wireless communication," in *ACM MOBICOM*, 2010, pp. 1–12.

[11] M. Duarte, C. Dick, and A. Sabharwal, "Experiment-driven characterization of full-duplex wireless systems," *IEEE Trans. Wireless Commun.*, vol. 11, no. 12, pp. 4296–4307, 2012.

[12] E. Tsakalaki, E. Foroozanfard, E. De Carvalho, and G. F. Pedersen, "A 2-order MIMO full-duplex antenna system," in *IEEE European Conf. Antennas and Propagation (EuCAP)*, 2014.

[13] A. Sahai, G. Patel, and A. Sabharwal, "Pushing the limits of full-duplex: Design and real-time implementation," *arXiv preprint arXiv:1107.0607*, 2011.

[14] E. Everett, A. Sahai, and A. Sabharwal, "Passive self-interference suppression for full-duplex infrastructure nodes," *IEEE Trans. Wireless Commun.*, vol. 13, no. 2, pp. 680–694, 2014.

[15] C. J. Kikkert, "Coupling," in *Power Line Communications: Principles, Standards and Applications from Multimedia to Smart Grid*, L. Lampe, A. Tonello, and T. Swart, Eds. John Wiley and Sons Ltd, 2016, ch. 4, pp. 223 – 260.

[16] D. Bharadia, E. McMilin, and S. Katti, "Full duplex Radios," in *ACM SIGCOMM*, 2013, pp. 375–386.

[17] Y.-S. Choi and H. Shirani-Mehr, "Simultaneous transmission and reception: Algorithm, design and system level performance," *IEEE Trans. Wireless Commun.*, vol. 12, no. 12, pp. 5992–6010, 2013.

[18] M. Duarte and A. Sabharwal, "Full-duplex wireless communications using off-the-shelf radios: Feasibility and first results," in *44th Asilomar Conference on Signals, Systems and Computers (ASILOMAR)*. IEEE, 2010, pp. 1558–1562.

[19] M. Duarte, A. Sabharwal, V. Aggarwal, R. Jana, K. Ramakrishnan, C. W. Rice, and N. Shankaranarayanan, "Design and characterization of a full-duplex multiantenna system for wifi networks," *IEEE Trans. Veh. Tech.*, vol. 63, no. 3, pp. 1160–1177, 2014.

[20] J.-H. Lee, "Self-interference cancelation using phase rotation in full-duplex wireless," *IEEE Trans. Veh. Tech.*, vol. 62, no. 9, pp. 4421–4429, 2013.

[21] S. Haykin, *Adaptive filter theory*. Pearson Education India, 2007.

[22] Intersil ISL1571 datasheet. [Online]. Available: http://www.intersil.com/content/dam/Intersil/documents/isl1/isl1571.pdf

[23] H. A. Latchman, S. Katar, L. Yonge, and S. Gavette, *Homeplug AV and IEEE 1901: A Handbook for PLC Designers and Users*. Wiley-IEEE Press, 2013.

[24] "IEEE standard for broadband over power line networks: Medium access control and physical layer specifications," *IEEE Std 1901-2010*, pp. 1–1586, Dec 2010.

[25] F. J. Canete, J. Cortés, L. Díez, and J. T. Entrambasaguas, "A channel model proposal for indoor power line communications," *IEEE Comm. Mag.*, vol. 49, no. 12, pp. 166–174, 2011.

[26] "Homeplug AV specification, version 1.1," *HomePlug Powerline Alliance*, pp. 1 – 673, May 2007.

[27] L. Ding, "Digital predistortion of power amplifiers for wireless applications," Ph.D. dissertation, Georgia Institute of Technology, 2004.

[28] G. Marrocco, D. Statovci, and S. Trautmann, "A PLC broadband channel simulator for indoor communications," in *IEEE Intl. Symp. Power Line Commun. and Its Appl. (ISPLC)*, 2013, pp. 321–326.

[29] A. M. Tonello and F. Versolatto, "Bottom-up statistical PLC channel modeling—Part I: Random topology model and efficient transfer function computation," *IEEE Trans. Power Del.*, vol. 26, no. 2, pp. 891–898, 2011.

[30] G. Prasad, H. Ma, M. J. Rahman, F. Aalamifar, and L. Lampe. (2016) A cumulative power line noise generator. [Online]. Available: http://www.ece.ubc.ca/∼gauthamp/PLCnoise